# Investigation of the Effects of Multi-Layer Winding Structures in Two Pole Synchronous Reluctance Machines

Didem Tekgun
*Dept. of Electrical & Electronics Engineering*
*Abdullah Gul University*
Kayseri, TURKEY
didem.tekgun@agu.edu.tr

Muhammed Muhsin Cosdu
*Dept. of Electrical & Electronics Engineering*
*Abdullah Gul University*
Kayseri, TURKEY
muhammedmuhsin.cosdu@agu.edu.tr

Burak Tekgun
*Dept. of Electrical & Electronics Engineering*
*Abdullah Gul University*
Kayseri, TURKEY
burak.tekgun@agu.edu.tr

Irfan Alan
*Dept. of Electrical & Electronics Engineering*
*Abdullah Gul University*
Kayseri, TURKEY
irfan.alan@agu.edu.tr

2021 3rd Global Power, Energy and Communication Conference (GPECOM) | 978-1-6654-3512-3/21/$31.00 ©2021 IEEE | DOI: 10.1109/GPECOM52585.2021.9587567

***Abstract*— In this paper, a comparative study is performed between single, various double, and triple-layer winding structures to investigate the effects of the winding MMF harmonics and end winding length on the two-pole synchronous reluctance machines (SynRM). A two-step design approach is used including winding and geometry optimization using multi-objective differential evolution (MODE) algorithm. In the first stage, a Pareto front is obtained which determines the number of turns for each coil group for all winding configurations. Later in the second stage, three results are selected from the first stage to perform a geometric optimization to distinguish the effects of the THD and end winding length on the synchronous performance of a 4 kW two-pole SynRM. For the same average torque output, efficiency, mass, and the torque ripple of the selected designs are investigated and compared. Based on the analysis, it is concluded that rather than focusing on shortening the end winding length, reducing the MMF harmonics have a more positive effect on the machine performance as reduced harmonics resulted in efficiency improvement up to 2 points and torque ripple is reduced up to 8 points while having similar motor mass.**

***Keywords*— synchronous reluctance machine, winding MMF harmonics, end winding reduction***

## I. INTRODUCTION

All around the world, reducing energy consumption is the common goal for both protecting natural resources and saving considerable costs. Due to global warming, sustainable and green motor technologies should be consumed consciously. Electrical motors and drive systems` energy consumption corresponds to between 35% and 40% of electrical energy production as global [1], [2]. The demands of energy-saving direct the machine designers' attention to find compact and robust motors with high efficiency for constant speed applications, especially in the low and middle power ranges. Motors in this power range are mainly used for industrial, domestic, and irrigation water pumping systems. The water pump system's motors used for irrigation purposes contribute a major part of energy consumptions by electric motors [1].

Induction Machines (IM) are usually preferred as the submersible water pump motor due to their robustness, reliability, low cost, and line start capability. However, the efficiency of the IM is quite low, especially in submersible versions. High torque, high efficiency, Permanent Magnet Synchronous Machine (PMSM) solutions are available, but they lead to high cost and rare earth magnet dependency. Besides, the degradation of rare earth magnets is another problem that might require magnet renewal or re-magnetizing in some cases. A hybrid technology called Line Start Synchronous Reluctance Machine (LS-SynRM) is a strong alternative to the traditional induction machines since they have the capability to start without any drive due to the addition of the cage inserted into the rotor core. Additionally, the rotor copper losses are eliminated due to the absence of the rotor windings which leads to a significant reduction in the copper losses of the motor. Hence, LS-SynRMs can compete with the IMs in terms of low price and ruggedness while having higher efficiency. However, two major shortcomings of the Synchronous Reluctance Motors (SynRM); high torque ripple and low power factor exist [3]–[6]. Various SynRM's rotor design studies with multi-barriers are extensively presented and discussed in the literature targeting torque ripple minimization [5] and improvement on the power factor [6]. In addition, several finite element analysis (FEA)-based multi-objective optimization methods for SynRM are reported in [7]–[9]. However, in the aforementioned studies, the stator winding configurations were kept as same as in IMs.

The negative impact of air-gap magneto-motive force (MMF) harmonics in an electrical machine has been extensively covered in the literature. The harmonics in the air-gap MMF are called space harmonics. Air-gap flux with space harmonics induces excessive copper and core losses in addition to vibration and acoustic noise [10]–[12]. A proper configuration of stator windings with reduced MMF space harmonic content leads to improve the overall machine performance significantly [13]–[16].

Since space harmonics inherently cause the non-sinusoidal winding distribution, having more sinusoidal back EMF waveforms with goals including less torque ripple, and power factor improvement is subject to the optimization problems of the two major winding types; distributed windings [13], [17], and fractional-slot concentrated windings (FSCWs) [16], [18].

Current researches in the literature have reported several studies on SynRMs with concentrated wound windings [19]. Non-overlapping, short end-turn length, high slot fill factor, and easier manufacturing are the important advantages of concentrated windings. However, the existing works on concentrated windings reveal that air-gap MMF harmonics are increased in these winding structures. These space harmonics lead to a higher torque ripple, the reduced power factor, the increased core and copper losses, and accordingly lower efficiency [19], [20]. To obtain reduced space harmonics a variety of three-phase winding configurations are proposed in [5], [21], [22]. Although the $5^{th}$ order harmonic improved the torque production, additional $7^{th}$, $17^{th}$, and $19^{th}$ order harmonics started to appear which degrades the performance of the machine. Therefore, the machine pole number and number of stator slots had to be increased [21], [22]. The core losses and fundamental frequency increase

978-1-6654-3512-3/21/$31.00 ©2021 IEEE

while the power factor reduces with an increased number of poles accordingly [23].

In addition to distributed windings and (FSCWs) another type of multilayer (ML) winding configuration for SynRM is reported in [24], which reduced torque ripple and torque per copper loss, and improved the power factor compared to the conventional winding structure. This winding scheme provides shorter end winding lengths and provides low THD MMF while keeping the pole number the same as in the distributed windings. The proposed ML winding configuration is applied to a 4 pole SynRM, after optimizing the rotor the machine efficiency is improved by 3.9% compared to conventional double-layer (DL) IMs.

In this paper, an investigation of various winding structures on the multi-objective design optimization of a 4 kW, 2 pole LS-SynRM's synchronous performance is presented. Single-layer, double layer, and triple-layer winding structures with an uneven number of turns on each coil are applied to a 24-slot stator. A two-step optimization study is performed namely winding optimization and geometry optimization. Firstly, the total harmonic distortion (THD) and an end winding score (EWS) of all the winding structures are calculated and optimized with multi-objective differential evolution (MODE) algorithm to get Pareto frontier designs. The result of this optimization shows what will be the best THD and EWS can be obtained in each winding configuration by distributing the coil number of turns in different percentages. Later, three different designs are selected from the obtained Pareto front for each winding structure and a geometric rotor optimization is performed for a 7 flux barrier rotor structure with maximum efficiency and minimum motor mass are being the objectives. After the rotor optimizations, a new set of Pareto frontier designs are obtained, which provided insights into how the machine efficiency and motor mass are affected by the MMF harmonics and shorter end windings. The results show that for all winding configurations, rather than reducing the end winding length reducing the THD of the MMF leads to higher quality Pareto fronts, and although the triple-layer winding has the best results, from the manufacturing standpoint, it is more practical to use a double layer version which has a similar performance to the triple-layer winding structure. As a result, the efficiency of the SynRM can go up to 93%, 92% with triple and double-layer windings, respectively. Comparing with the conventional IMs at the same power level, the machine efficiency class is improved from standard efficiency IE1 to ultra-premium efficiency IE4.

## II. Methodology

### A. Winding Optimization

In order for a SynRM to rotate around 3000 r/min with a 50 Hz AC power line voltage, it should have a configuration of 2 poles. However, in this configuration having only single-layer winding per slot both increases the length of the end winding and increases the THD. In order to lower THD and decrease total winding length, a single layer conventional winding, four different double-layer winding, and one three-layer winding configuration are tested. These configurations are shown in Fig. 1.

For the determination of the number of turns of each loop in a phase, an optimization problem is defined to find optimal winding distributions. Optimization parameters are set as proportional values for each loop with a total of 1, in order to make them proportional to the total number of turns explained in the geometric optimization. The optimization has two objectives which are THD and EWS, the calculations of these values are formulated in (1) through (5) [25].

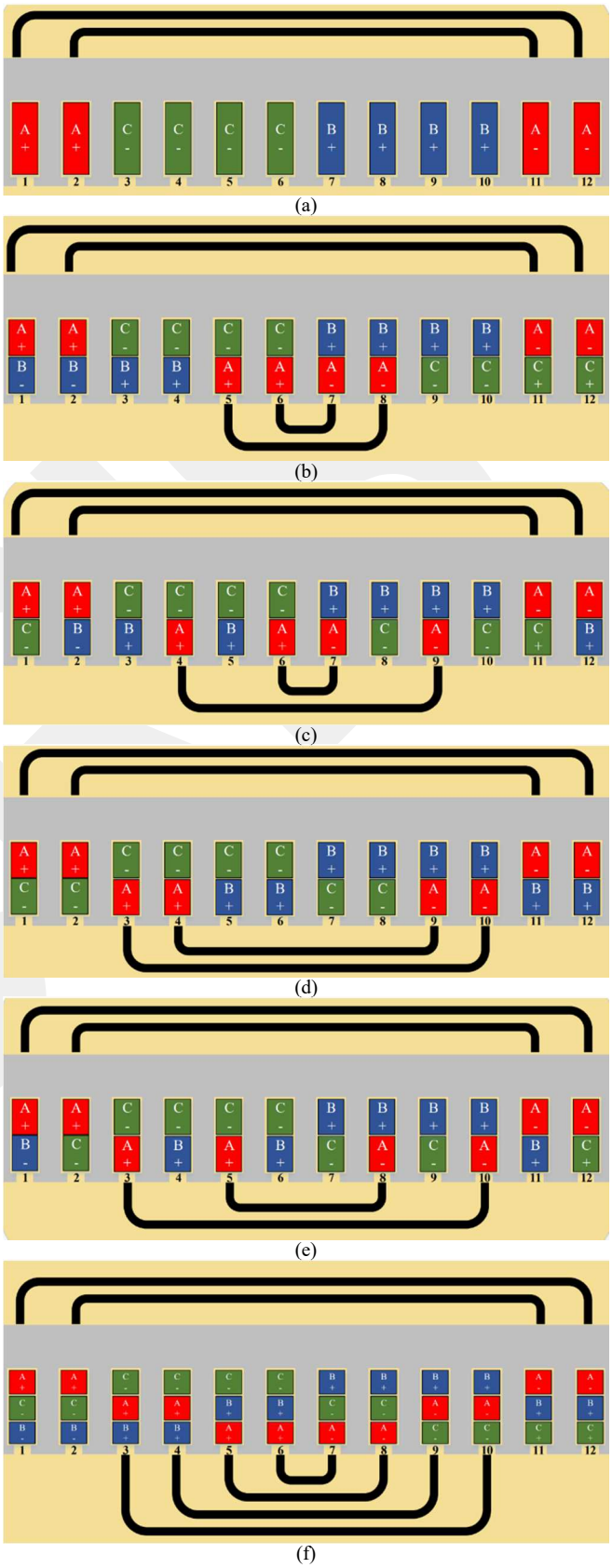


Fig. 1. Visual representation of the (a) single layer, (b) double-layer version 1, (c) double-layer version 2, (d) double-layer version 3, (e) double-layer version 4 and (f) triple-layer winding configurations.

$$k_{pv} = \frac{1}{N_{ph}} \sum_{n} N_n . q_n . \sin(v . \frac{2n-1}{\tau_p} . \frac{\pi}{2}) \quad (1)$$

$$N_{ph} = \sum_{n} N_n . q_n \quad (2)$$

$$F_{st} = \frac{3}{\pi . v} . \frac{N_{ph}}{p} . k_{pv} . i_s \quad (3)$$

$$THD = \frac{\sqrt{\left(F_{st}{}^{5}\right)^2 + \left(F_{st}{}^{7}\right)^2 + \left(F_{st}{}^{11}\right)^2 + \left(F_{st}{}^{13}\right)^2 + \cdots}}{F_{st}{}^{1}} = \frac{\sqrt{(\sum_{m=1}^{6}) . (F_{st}{}^{6m\pm1})^2}}{F_{st}{}^{1}} \quad (4)$$

$$EWS = \sum_{n} \frac{l_{arc,n}}{l_{WP}} k_n \quad (5)$$

Here, $k_{pv}$ is the pitch factor, $N_{ph}$ is the total number of turns per phase, $N_n$ is the number of turns for the coil group, $q_n$ is the coil groups per pole pair, $\tau_p$ is the pole pitch, $F_{st}$ is the peak value of the harmonics, $i_s$ is the peak value of the current, $v$ is the harmonic order number that is equal to (1 ± 6c), where c is a natural number for the MMF distribution of a balanced three-phase machine, $n$ is the number of coils, $l_{arc,n}$ is the arc length of the $n^{th}$ coil group, $l_{WP}$ is the perimeter of the circle that passes through the mid-points of the stator slots, and $k_n$ is the proportional coefficient of the $n^{th}$ coil group.

### *B. Geometric Optimization*

Although conducting a winding optimization based on analytical calculation gives some intuition about the outcomes, a geometric optimization based on FEA analysis is also required for acquiring more accurate results. Since conducting a geometric optimization takes quite a computational work, three variations are selected for each winding configuration which represents minimum THD, minimum EWS, and a middle point between these two objectives. In order to perform a geometric optimization, an FEA model is created in ANSYS Maxwell 2D. For the initial model, many geometric definitions decrease the efficiency of the optimization. To increase the optimization efficiency, the number of geometric design parameters is reduced to seven parameters which are highly effective on the output parameters. Graphical representations of these parameters are shown in Fig. 2 and related explanations are given in Table I.

Furthermore, in order to find the best possible results with respect to the objectives, a variety of working conditions should be tested. For conducting such analysis, some non-geometric parameters current density and the maximum current is also added as a parameter to the optimization.

Parameters regarding the stator shape are set to a fixed value due to manufacturing and compatibility concerns. A 24-slot stator configuration is used for this project. Motor outer radius ($r_{MO}$) is specified as 68 mm since the motor is expected to mount inside the water pump system. In addition, stator inner radius is appointed as 34 mm, tooth width parameter ($l_{TW}$) is taken as 3.2 mm and slot depth parameter ($l_{SD}$) is set to 20.5 mm. Two other predetermined parameters were the airgap (g) which is fixed at 0.35 mm and rotor outer clearance ($l_{OC}$) determined as 0.5 mm due to producing maximum torque within the production limits. There are two dependent parameters that are not shown in Table I. One of them is the stack length. Since the motor is expected to provide 4kW output power with a rotation speed of 3000 r/min with 50 Hz supply, 14 Nm torque is required to be generated. In order to fix the average output torque of the motor, first, stack length is taken as 25 mm, and the torque is calculated considering this length, then, by FEA software and then the stack length linearly scaled for providing 14 Nm torque.

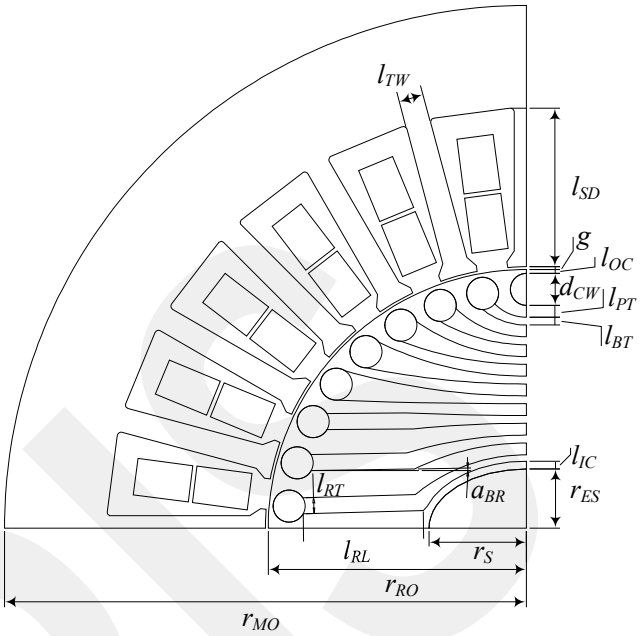


Fig. 2. Visual representation of geometric design parameters.

TABLE I. OPTIMIZATION PARAMETERS

| Design Parameter | Definition | Boundaries |
|---|---|---|
| $a_{BR}$ [degree] | Angle of the rectangular section of the bars | 0 – 10 |
| $l_D$ [mm] | Shaft Radius ($r_S$) $-$ *Elliptic Shaft Radius* ($r_{ES}$) | 0 – 5 |
| $l_{IC}$ [mm] | The thickness of the Shaft Clearance | 1 – 5 |
| $k_B$ | $\frac{\text{MidPoint Bar Thickness } (l_{BT})}{\text{MidPoint Plate Thickness } (l_{PT})}$ | 0.16 – 0.6 |
| $k_C$ | $\frac{\text{Cage Cylinder Diameter } (d_{CW})}{\text{Maximum Possible Cage Diameter}}$ | 0.67 – 0.85 |
| $k_R$ | $\frac{\text{Rectangular Bar Length } (l_{RL})}{\text{Maximum Possible Length}}$ | 0.5 – 0.9 |
| $k_{REC}$ | $\frac{\text{Rectangular Bar Thickness } (l_{RT})}{\text{Cage Cylinder Diameter } (d_{CW})}$ | 0.35 – 0.75 |
| $J$ [A/mm$^2$] | Current density | 3 – 10 |
| $I_{peak}$ [A] | Peak Current | 5 – 15 |

The second parameter is the number of turns of the coils. For the sake of getting the highest torque possible from the motor, the number of turns, $N_t$, is calculated based on the RMS value of the current, $I_{rms}$, current density, $J$, and the slot area, $A_{slot}$ as in (6) for each variation. Due to manufacturing limitations, fill factor, $k_{fill}$, is selected as 0.35.

$$N_t = \frac{J \times I_{rms}}{A_{slot} \times k_{fill}} \quad (6)$$

The optimization algorithms work based on a cost definition which has several objectives and constraints. Efficiency and torque density are selected as the objectives of this optimization. However, due to the fact that the average torque value is predetermined (14 Nm at a speed of 3000 r/min), the second objective is simplified to motor mass. Also, in order to be able to operate with the line voltage, the

motor terminal voltage has to be within the 5% band of the actual line voltage amplitude. Hence, the motor terminal voltage and torque ripple are set as constraints. Furthermore, motor mass was also added to constraints to get more manufacturable results from the optimization. The calculation methods and limits of these constraints are shown in Table II.

TABLE II. CONSTRAINTS

| Design Constraint | Calculation Method | Boundaries |
|---|---|---|
| Line Voltage | $\max(Induced\ Voltage) + I_{Rms} * r_{copper}$ | 310 – 340 (V) |
| Torque Ripple | $\frac{\text{Peak To Peak Torque}}{\text{Average Torque}} \times 100$ | 0% – 50% |
| Motor Mass | (Area (Stator) + Area (Rotor)) ×Stack Length + Copper Mass | 0 – 25 (kg) |

### C. Optimization Algorithm

In this study, the improved MODE algorithm introduced in [26] is used for the geometric optimization of the motor as well as the windings. The general working principle of the algorithm is demonstrated in Fig. 3. The process begins with generating a random parent, then solves the parent vector with FEA. Following that step, the optimization performs a population increase check and if population size (PopS) is smaller than the maximum allowed size (MPS) and generation number (GenN) is larger than a predetermined generation number (BPS), it increases the size of the mutant vector. After these steps, the child vector is created by crossing over between mutant and parent vector. Then, the solutions for the child vector are acquired with FEA software and these results are compared with the parent in the selection process. Qualified results are picked for the new parent and Pareto front. If the retraction condition is fulfilled (GenN == PRV×k, k ϵ ℕ, where PRV is predetermined number of generations to carry out a retraction process), the results kept in the Pareto Front update parent vector with respect to the dominance filter. Otherwise, the output of the selection algorithm directly creates the new parent vector. Until the generation number reaches the maximum number (MaxGen) the algorithm works in the loop to find a Pareto distribution between objectives having a trade-off between them. A detailed explanation of the optimization method can be found in [26]. Due to the page limitations and the paper's focus is being the investigation of the MMF harmonics and end winding lengths on the machine performance, a detailed explanation of the altered MODE is not covered in this paper.

## III. RESULTS & DISCUSSION

In this study, six different winding configurations are tested for their harmonic distribution and end winding length. Since both of these parameters are quite effective on motor performance, a distribution is found considering these parameters using a MODE algorithm. The results of winding optimization with different winding configurations are presented in Fig. 4.

The results indicate that there is a trade-off between THD and EWS. However, the motor geometry is also a determinant in the machine performance. Therefore, three results from different winding configurations are selected where the THD is minimum, EWS is minimum at 20 % THD limit, and a mid-point between the minimum THD and minimum EWS for geometric optimization. The reason for these selections is to distinguish the effects of the harmonic reduction and end winding length reduction on the machine efficiency, mass, and torque ripple.

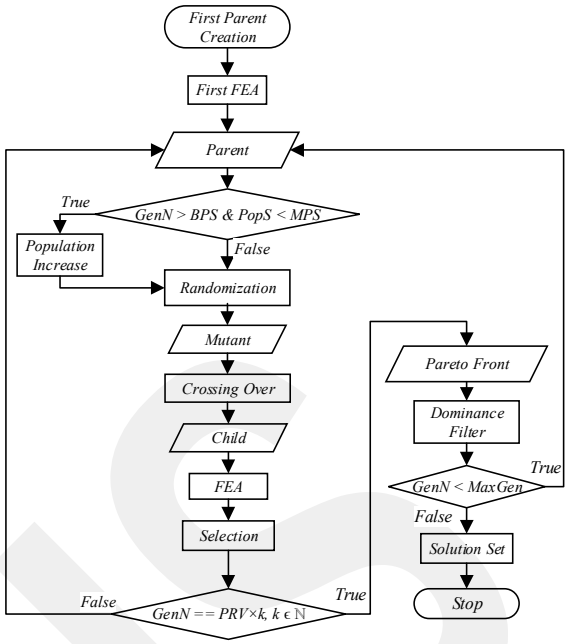


Fig. 3. Flowchart of Altered MODE algorithm, adapted from [26, Fig. 1].

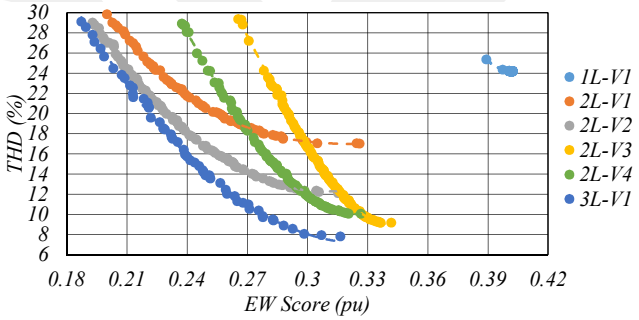


Fig. 4. THD and EWS results of different winding configurations.

The geometric optimization results of the single layer, double layer versions 1, 2, 3, and 4, and triple-layer winding configurations are presented in Fig. 5.a, Fig. 5.b, Fig. 5.c, Fig. 5.d, Fig. 5.e, and Fig. 5.f, respectively. The color scheme of these graphs placed on top is arranged to demonstrate their torque ripple.

When the results of the different winding configurations are compared, it can be seen that the double layer version 3 and triple-layer configurations have better results than the single-layer base configuration for the whole distribution. The graph demonstrates when the torque density increase results in a decrease in the motor mass, some winding configurations can provide up to a 2% efficiency increase. When the middle section of the distributions is examined, the efficiency increase changes between 0.4% and 1%; however, a significant decrease in the torque ripple is observed, which is around 3% for the double layer version 3 and 8% for the triple-layer configurations. This outcome is also effective in the noise and vibration performance of the machine which leads an improved reliability and life cycle of the machine.

The results show that minimizing THD yields higher efficiency, lower torque ripple, and lower motor mass. On the other hand, reducing the end winding length provides copper loss reduction up to a point where the THD levels exceed a certain level that results in a decrease in torque production.

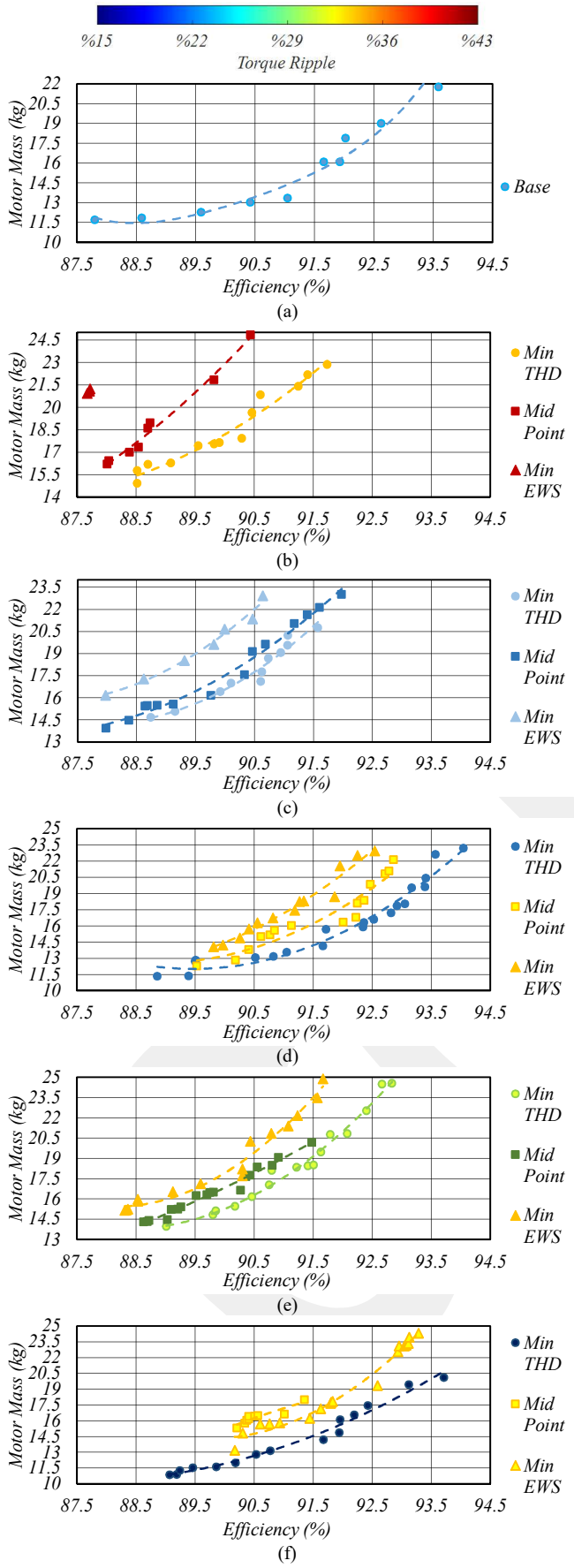


Fig. 5. Geometric optimization results of the (a) single-layer, (b) double-layer version 1, (c) double-layer version 2, (d) double-layer version 3, (e) double-layer version 4 and (f) triple-layer winding configurations.

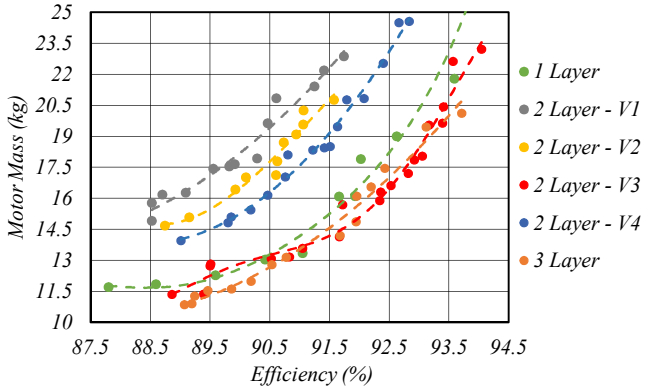


Fig. 6. Comparison of optimization results for different winding configurations.

From the results demonstrated in Fig. 5, it can be concluded that winding configurations that favor for minimization of THD yield better results in comparison with the configurations that minimize EWS. This finding is parallel with the expectations since SynRM is highly affected by the magnetic field distribution. Minimum THD configurations for every winding scheme are given in Fig. 6 as they have better Pareto frontiers than others. The color scheme of these plots is not arranged with respect to torque ripple to eliminate confusion between results.

When the results of the different winding configurations are compared, the triple-layer and the 3rd version of the double-layer configurations have higher quality results than the single-layer configuration for the whole distribution.

## IV. Conclusions

In this paper, an investigation of the multilayer winding structures that have an uneven number of turns on each coil group on various performance parameters of a 2 pole line start synchronous reluctance machine is provided. Single-layer, four different versions of double-layer, and triple-layer winding structures are considered for a 24 slot stator. The analysis is performed in two stages. First, a winding optimization that determines each coil group's number of turns percentage to the total number of turns per phase with the objectives of minimizing the THD of the winding MMF and a score that indicates the total end winding length. This process is done with multi-objective differential evolution (MODE) algorithm for all the winding configurations. Later a geometric optimization is performed using three winding optimization results which are having the minimum THD, minimum end winding score at a maximum of 20 % THD, and a point in between these two from each winding configuration. The reason for selecting these three results is to distinguish the effects of the MMF harmonics and the end winding length on the performance of the machine. This second optimization is performed for the given conditions and Pareto optimal designs are determined and compared in terms of efficiency, mass, and torque ripple. Among all the winding structures, the triple-layer winding structure yielded the highest quality results. Considering the manufacturing complexity and cost, version 3 of the double-layer winding structure is found to have similar results to the triple windings. Moreover, it is also concluded that in synchronous reluctance machine designs, winding MMF THD is more effective than reducing the end winding turns hence the copper loss. Better MMF distribution leads to higher torque production, smaller machine size, and lower torque ripple.

## ACKNOWLEDGMENT

This research is supported by The Scientific and Technological Research Council of Turkey (TUBITAK) under Grant 118E172.

## REFERENCES

[1] A. T. De Almeida, S. Member, F. J. T. E. Ferreira, and S. Member, "Beyond Induction Motors — Technology Trends to Move Up Efficiency," vol. 50, no. 3, pp. 2103–2114, 2014.

[2] K. Tang, L. Zhou, J. Wang, Y. Xiao, and S. Wang, "Rotor design and optimization of the single-phase line-start synchronous reluctance motor," in *2017 20th International Conference on Electrical Machines and Systems (ICEMS)*, 2017, pp. 1–4.

[3] N. Bianchi, S. Bolognani, D. Bon, and M. D. Pré, "Rotor flux-barrier design for torque ripple reduction in synchronous reluctance and PM-assisted synchronous reluctance motors," *IEEE Trans. Ind. Appl.*, vol. 45, no. 3, pp. 921–928, 2009.

[4] T. A. Lipo, "Synchronous reluctance machines-a viable alternative for ac drives?," *Electr. Mach. Power Syst.*, vol. 19, no. 6, pp. 659–671, 1991.

[5] A. Vagati, M. Pastorelli, G. Franceschini, and S. C. Petrache, "Design of low-torque-ripple synchronous reluctance motors," *IEEE Trans. Ind. Appl.*, vol. 34, no. 4, pp. 758–765, 1998.

[6] H. Kim *et al.*, "A study on the rotor design of line start synchronous reluctance motor for ie4 efficiency and improving power factor," *Energies*, vol. 13, no. 21, 2020.

[7] F. Cupertino, G. Pellegrino, and C. Gerada, "Design of synchronous reluctance motors with multiobjective optimization algorithms," *IEEE Trans. Ind. Appl.*, vol. 50, no. 6, pp. 3617–3627, 2014.

[8] H. Shao, C. Zhong, T. G. Habetler, and S. Li, "Multi-Objective Design Optimization of Synchronous Reluctance Machines Based on the Analytical Model and the Evolutionary Algorithms," *51st North Am. Power Symp. NAPS 2019*, 2019.

[9] S. Sato, T. Sato, and H. Igarashi, "Topology optimization of synchronous reluctance motor using normalized gaussian network," *IEEE Trans. Magn.*, vol. 51, no. 3, 2015.

[10] K. Kurihara, G. Wakui, and T. Kubota, "Steady-State Performance Analysis of Permanent I "," *IEEE Trans. Magn.*, vol. 30, no. 3, pp. 1306–1315, 1994.

[11] G. Dajaku, W. Xie, and D. Gerling, "Reduction of low space harmonics for the fractional slot concentrated windings using a novel stator design," *IEEE Trans. Magn.*, vol. 50, no. 5, 2014.

[12] G. Dajaku, S. Spas, and D. Gerling, "Advanced optimization methods for fractional slot concentrated windings," *Electr. Eng.*, vol. 101, no. 1, pp. 103–120, 2019.

[13] D. A. Kocabas, "Novel winding and core design for maximum reduction of harmonic magnetomotive force in AC motors," *IEEE Trans. Magn.*, vol. 45, no. 2, pp. 735–746, 2009.

[14] T. Gundogdu and G. Komurgoz, "Investigation of winding MMF harmonic reduction methods in IPM machines equipped with FSCWs," *Int. Trans. Electr. Energy Syst.*, vol. 29, no. 1, pp. 1–27, 2019.

[15] I. Petrov, P. Ponomarev, Y. Alexandrova, and J. Pyrhonen, "Unequal Teeth Widths for Torque Ripple Reduction in Permanent Magnet Synchronous Machines With Fractional-Slot Non-Overlapping Windings," *IEEE Trans. Magn.*, vol. 51, no. 2, 2015.

[16] A. M. EL-Refaie, "Fractional-slot concentrated-windings synchronous permanent magnet machines: Opportunities and challenges," *IEEE Trans. Ind. Electron.*, vol. 57, no. 1, pp. 107–121, 2010.

[17] T. Hamiti, T. Lubin, L. Baghli, and A. Rezzoug, "Modeling of a synchronous reluctance machine accounting for space harmonics in view of torque ripple minimization," *Math. Comput. Simul.*, vol. 81, no. 2, pp. 354–366, 2010.

[18] G. Dajaku and D. Gerling, "Different novel methods for reduction of low space harmonics for the fractional slot concentrated windings," *ICEMS 2012 - Proc. 15th Int. Conf. Electr. Mach. Syst.*, 2012.

[19] C. M. Spargo, B. C. Mecrow, and J. D. Widmer, "Application of fractional slot concentrated windings to synchronous reluctance machines," *Proc. 2013 IEEE Int. Electr. Mach. Drives Conf. IEMDC 2013*, pp. 618–625, 2013.

[20] M. Gamba, G. Pellegrino, and A. Vagati, "A new PM-assisted synchronous reluctance machine with a nonconventional fractional slot per pole combination," *J. Electr. Eng.*, vol. 15, no. 1, pp. 97–104, 2015.

[21] M. V. Cistelecan, F. J. T. E. Ferreira, and M. Popescu, "Three phase tooth-concentrated multiple-layer fractional windings with low space harmonic content," *2010 IEEE Energy Convers. Congr. Expo. ECCE 2010 - Proc.*, pp. 1399–1405, 2010.

[22] G. Dajaku and D. Gerling, "A Novel 24-Slots/10-Poles Winding Topology for Electric Machines," *2011 IEEE Int. Electr. Mach. Drives Conf. IEMDC 2011*, pp. 65–70, 2011.

[23] M. A. Kabir and I. Husain, "New multilayer winding configuration for distributed MMF in AC machines with shorter end-turn length," *IEEE Power Energy Soc. Gen. Meet.*, vol. 2016-Novem, pp. 0–4, 2016.

[24] M. A. Kabir and I. Husain, "Application of a Multilayer AC Winding to Design Synchronous Reluctance Motors," *IEEE Trans. Ind. Appl.*, vol. 54, no. 6, pp. 5941–5953, 2018.

[25] J. Pyrhönen, T. Jokinen, and V. Hrabovcová, *Design of Rotating Electrical Machines*. 2008.

[26] M. M. Cosdu, A. F. Hacan, and B. Tekgun, "Design Optimization of an Outer Rotor PMSM for a Drive Cycle using an Improved MODE Algorithm for a Lightweight Racing Vehicle," *Proc. - 2020 6th Int. Conf. Electr. Power Energy Convers. Syst. EPECS 2020*, pp. 58–63, 2020.